First In Vivo Application of
Microwave Radiometry in Human Carotids

A New Noninvasive Method for
Detection of Local Inflammatory Activation

Konstantinos Toutouzas, MD,* Charalampos Grassos, MD,* Maria Drakopoulou, MD,*
Andreas Synetos, MD,* Eleftherios Tsiamis, MD,* Constantina Aggeli, MD,*
Konstantinos Stathogiannis, MD,* Dimitrios Klettas, MD,* Nikolaos Kavantzas, MD,†
Georgios Agrogiannis, MD,† Efstratios Patsouris, MD,† Christos Klonaris, MD,‡ Nikolaos Liasis, MD,*
Dimitrios Tousoulis, MD,* Elias Siores, BSc, MSc, PhD,§ Christodoulos Stefanadis, MD*

Athens, Greece; and Bolton, United Kingdom

Objectives	This study investigated whether temperature differences: 1) can be measured in vivo noninvasively by microwave radiometry (MR); and 2) are associated with ultrasound and histological findings.
Background	Studies of human carotid artery samples showed increased heat production. MR allows in vivo noninvasive measurement of internal temperature of tissues.
Methods	Thirty-four patients undergoing carotid endarterectomy underwent screening of carotid atherosclerosis by ultrasound and MR. Healthy volunteers were enrolled as a control group. During ultrasound study, plaque texture, plaque surface, and plaque echogenicity were analyzed. Temperature difference (ΔT) was assigned as maximal minus minimum temperature. Association of thermographic with ultrasound and histological findings was performed.
Results	ΔT was higher in atherosclerotic carotid arteries compared with the carotid arteries of controls ($p < 0.01$). Fatty plaques had higher ΔT compared with mixed and calcified ($p < 0.01$) plaques. Plaques with ulcerated surface had higher ΔT compared with plaques with irregular and regular surface ($p < 0.01$). Heterogeneous plaques had higher ΔT compared with homogenous ($p < 0.01$). Specimens with thin fibrous cap and intense expression of CD3, CD68, and vascular endothelial growth factor (VEGF) had higher ΔT compared with specimens with thick cap and low expression of CD3, CD68, and VEGF ($p < 0.01$).
Conclusions	MR provides in vivo noninvasive temperature measurements of carotid plaques, reflecting plaque inflammatory activation. (J Am Coll Cardiol 2012;59:1645–53) © 2012 by the American College of Cardiology Foundation

Atherosclerosis is the main cause of ischemic stroke, and recent studies have shown that even low-grade stenosis may lead to the development of cerebrovascular events (1–4). Thus, the identification of other high-risk features of plaques could lead to decreases in the incidence of strokes, especially in patients with asymptomatic carotid artery disease.

The role of inflammation in destabilizing carotid plaques has been recognized (5,6). Previous studies have shown that carotid plaques had increased density of inflammatory cells producing increased thermal heterogeneity (7). For the evaluation of plaque inflammatory status, novel imaging techniques have emerged (8–12). However, no method is currently available for the in vivo noninvasive measurement of carotid plaque temperature.

Microwave radiometry (MR) is based on the ability to detect noninvasively, with high accuracy, relative changes of temperature in human tissues (13–16). MR measures natural electromagnetic radiation from internal tissues at microwave frequencies, and the intensity of the radiation is proportional to the temperature of the tissue. MR has already been applied in oncology (17). Recently, the safety

and effectiveness of MR in plaques have been demonstrated in an experimental model (18).

The aim of the present study was to investigate whether temperature differences in patients with carotid arteries: 1) can be measured in vivo noninvasively by MR; and 2) are associated with ultrasound and histological findings.

Methods

Study population. Consecutive patients with either symptomatic or asymptomatic single high-degree carotid artery stenosis (>80% to 85%) who were scheduled for carotid endarterectomy were enrolled prospectively in the study. All patients underwent evaluation of carotid atherosclerosis by ultrasound and MR blindly by 2 different operators within 1 week before the scheduled operation. The control group consisted of 15 healthy volunteers without carotid artery disease documented by carotid ultrasound.

Epidemiological data, neurological symptoms, vascular risk factors, and current therapy were recorded. Hypertension was defined by systolic blood pressure >140 mm Hg and/or diastolic blood pressure >90 mm Hg or by taking prescribed antihypertensive medications. Dyslipidemia was defined as an elevation of plasma low-density lipoprotein cholesterol >160 mg/dl, plasma triglycerides >200 mg/dl, both, or a high-density lipoprotein level <40 mg/dl for men and <50 mg/dl for women (19). Diabetes mellitus was defined by the presence of fasting plasma glucose >126 mg/dl and/or hemoglobin A1c >6.4% or by taking antidiabetic treatment.

Patients with recent (<6 months) cardiological ischemic events; history of vasculitis; nonatherosclerotic carotid artery disease; or intermittent inflammatory, infectious, or neoplastic conditions were excluded from the study. All patients gave written informed consent.

Ultrasound imaging and analysis. Extracranial carotid arteries were examined with an ultrasound unit (Logic 9, 6-9 MHz transducer, GE Healthcare, Waukesha, Wisconsin). All data were collected and interpreted by 2 experienced ultrasonographers (C.A. and N.L.). In case of disagreement, the patient had to be excluded; however, the 2 operators agreed on all classifications.

The ultrasound protocol included evaluation of the carotid arteries from their point of origin; the subclavian, vertebral, and innominate arteries including the common carotid arteries throughout their whole length; and the internal and external carotid arteries extracranially in transverse and longitudinal sections. B-mode ultrasound was used to evaluate atheromatic plaque morphology and consistency. Plaques were evaluated for the following main parameters: echogenicity, consistency, and surface contour.

To assess plaque echogenicity, the following classification was used: echolucent plaques with echogenic fibrous caps were classified as type I; plaques predominantly hypoechogenic with echolucent areas representing <25% of the plaque were classified as type II; hyperechogenic plaques with <20% echolucency were classified as type III; echogenic homogeneous plaques were classified as type IV; and type V were highly echogenic plaques that produced posterior acoustic shadowing (8,20).

We considered types I and II as fatty plaques, types III and IV as mixed plaques, and type V as calcified plaques (21). We further categorized fatty plaques as heterogeneous and mixed and calcified as homogeneous according to previous classification (20,21).

The plaque surface was considered regular when it was smooth, irregular if a variation between 0.3 and 0.9 mm was observed on the surface of the plaque with depth >1 mm, and ulcerated if an irregularity or break was observed on the surface of the plaque with depth >1 mm and width >2 mm (22).

MR measurements. The MR measurements were performed with a microwave computer-based system (RTM 01 RES, Bolton, United Kingdom) that detects temperature from internal tissues at microwave frequencies. The basic
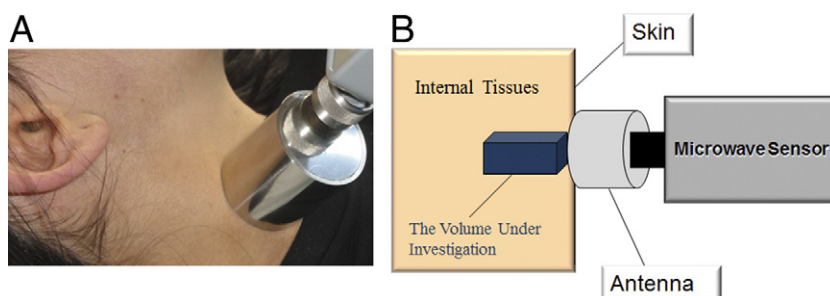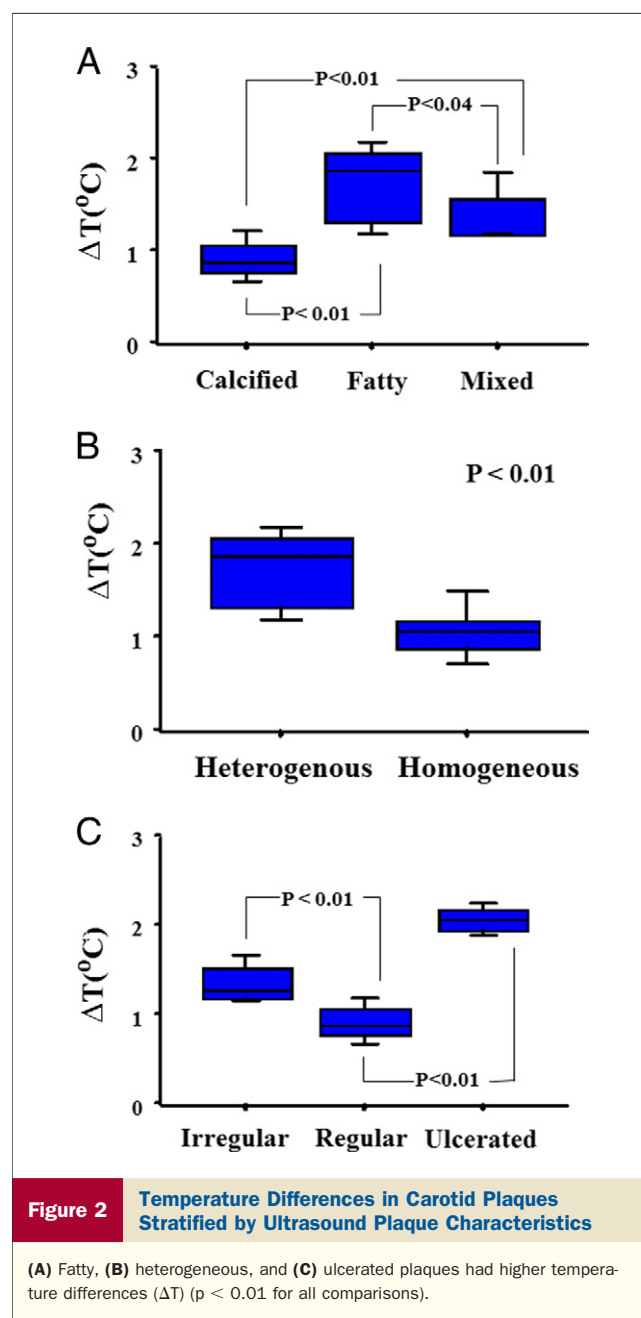

Figure 1   **Microwave Radiometry**

(A) Photograph of the antenna for microwave radiometry measurements placed at a 90° angle. **(B)** Schematic presentation of the system of microwave radiometry. The antenna of the microwave sensor is in contact with the skin above the volume under investigation.

principles of MR have been previously described (13,14). Briefly, the fundamental basis for a microwave imaging technique is the significant contrast in the dielectric properties at microwave frequencies of different tissues. The depth of penetration depends on the wavelength, the dielectric properties, and the water content of the tissue. The system of MR possesses an antenna with 2 sensors: a microwave and an infrared. The microwave sensor is 3.9 cm in diameter and detects microwave radiation at 2 to 5 GHz, which corresponds to ≤7 cm in depth, with an accuracy for temperature measurements of ±0.20°C. The sensor blocks all microwave signals from the environment. The "volume under investigation" has a rectangular area of 3 cm in width, 2 cm in length, and 3 to 7 cm in depth depending on the dielectric properties of the underlying tissues (23). The second sensor is used for infrared measurements from the skin, for calibrating the microwave sensor readings.

To ensure that matching cross-sections were compared between ultrasound and MR, the measurements were performed starting transversely from the proximal common carotid artery and moving distally based on markers located under the guidance of ultrasound. For this purpose, the common carotid bifurcation, defined as the last cross-section with a single common carotid artery lumen, was used as an internal marker. MR measurements were also performed 2 cm proximal and 2 cm distal to the bifurcation region. Palpation or ultrasound study of the carotid artery that could influence the temperature distribution was performed at least 10 min before the temperature measurement. During measurements, the microwave antenna of the device was placed in contact with the skin at a 90° angle (Fig. 1). The antenna was held at this position for 10 s, which is required for the receiver to integrate the microwave emission and the conversion of the measured signal to temperature by a microprocessor. The temperature data were displayed as a temperature field, in which cool areas of the vessel were displayed by "cold" colors (i.e., blue) and hot ones were reflected by "warm" colors (red and orange). The temperature field did not correspond to the orientation of the ultrasound images of the carotid arteries. All measurements of the carotid arteries were performed 3 times at each of the 3 segments to assess the reproducibility of the method (overall, 9 measurements by each operator) in a room temperature between 20°C and 24°C. The temperature of each segment used for further analysis was the mean of the 3 temperatures. The measurements were compared to study the intraobserver variability. The differences in the mean temperature in each segment measured by each operator were compared to study the interobserver variability. Temperature difference (ΔT) for each carotid artery was assigned as the maximal temperature minus the minimal temperature detected among carotid artery segments. The mean value of the 2 ΔTs calculated by the 2 different operators was used for the analysis of each carotid artery.

Histological analysis. Carotid plaques were removed in full to preserve the plaque structure. After 24 h of decalcification, samples were cut in serial sections, and the area with the highest percentage of stenosis was identified macroscopically and defined as the area of interest for further analysis. All samples were fixed in 10% buffered formalin for 24 h, decalcified overnight with formic acid, and processed for routine paraffin embedding. Each plaque was then divided radially, and 5-mm–thick sections were obtained from paraffin-embedded samples and stained with hematoxylin and eosin. Histological sections were analyzed semiquantitatively for inflammatory cells. An arbitrary 2-level score assigning "−" to the absence of or focal or

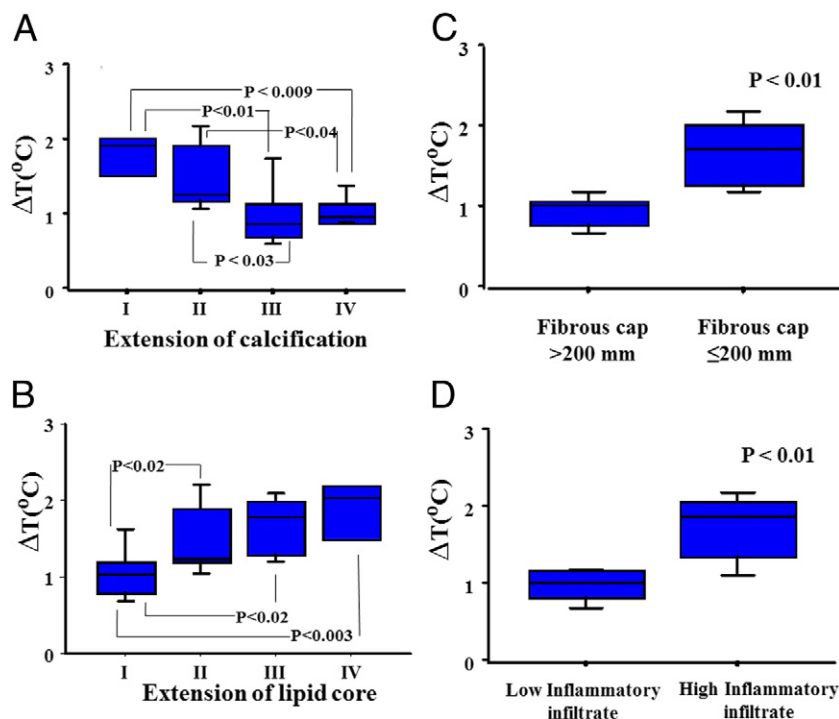**Figure 2** **Temperature Differences in Carotid Plaques Stratified by Ultrasound Plaque Characteristics**

(A) Fatty, **(B)** heterogeneous, and **(C)** ulcerated plaques had higher temperature differences (ΔT) (p < 0.01 for all comparisons).

Figure 3   Temperature Differences in Carotid Plaques Stratified by Histological Characteristics

Plaques with low extension of **(A)** calcification, **(B)** increased lipid core, **(C)** thin fibrous cap ($\leq 200\ \mu m$), and **(D)** inflammatory infiltrate had higher temperature differences (ΔT) (p < 0.01 for all comparisons).

circumscribed presence of inflammatory cells and "+" to their maximal expression was used (24).

Extent of calcification and lipid core was evaluated on the entire circumferential arterial sections dividing the field into 4 equal parts. According to previous classifications, we scored in numerical values ranging from 0 to 4 based on the extent of calcification and lipid core (0 = no calcification or core at all, 1 = one-quarter of the 4 equal parts showed calcification or core, 2 = one-half of the 4 equal parts, 3 = three-quarters of the 4 equal parts, and 4 = all of the 4 parts) (8). We used a cut-off value for cap thickness of 200 μm to categorize thick and thin fibrous caps (8).

Immunohistochemical analysis. CD68 was used as a macrophage marker, CD3 as a lymphocyte marker, and vascular endothelial growth factor (VEGF) as a marker of neoangiogenesis. The following primary antibodies were used: anti-CD3, (Dako, Glostrup, Denmark), anti-CD68, and anti-VEGF (Dako A/S, Copenhagen, Denmark). The positivity for each antibody was semiquantitatively scored as intense (3+), moderate (2+), low (2+), or absent (0+). For the analysis of a sample with a score <2 or ≥2, we attributed a value of 0 (low) or 1 (high), respectively (8).
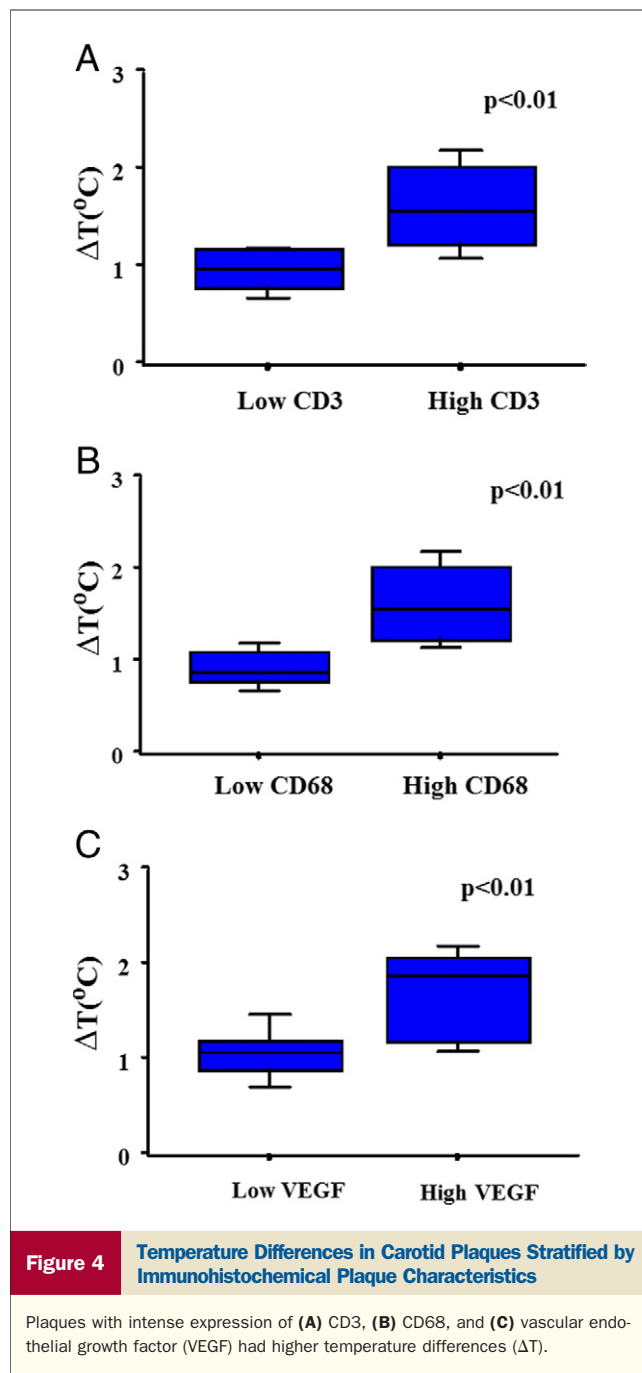
Statistical analysis. Statistical analysis was performed with commercially available software (SPSS Inc., Chicago, Illinois). Quantitative data are presented as rates or mean value ± SD. Probability values are 2-sided from the Student

unpaired *t* test for continuous variables, and analysis of variance was used for ≥3 groups (Figs. 2, 3, and 4). Correlation for intraobserver and interobserver measurements was assessed by the Pearson correlation test. A value of p < 0.05 was considered significant.

Results

Baseline demographic and clinical characteristics. Forty-four consecutive patients with significant carotid artery stenosis were included in the study. Ten patients who met the exclusion criteria were excluded from the study. The clinical characteristics of the 2 groups are summarized in Table 1. All carotid specimens were suitable for histology and immunohistochemical analysis. For measurements of the temperature in each segment by MR, both intraobserver (0.06°C ± 0.08°C; range 0 to 0.20°C) and interobserver (0.08°C ± 0.11°C; range 0 to 0.30°C) differences were lower than the accuracy of the microwave sensor (r = 0.94 for intraobserver and r = 0.89 for interobserver measurements).

Ultrasound analysis. Vertebral and innominate arteries were not diseased. ΔT was higher in atherosclerotic carotid arteries compared with the carotid arteries of controls (1.39°C ± 0.49°C vs. 0.23°C ± 0.01°C). Fatty plaques had higher ΔT compared with mixed and calcified plaques (p < 0.01) (Fig. 2A). Heterogeneous plaques with ulcerated

Figure 4 **Temperature Differences in Carotid Plaques Stratified by Immunohistochemical Plaque Characteristics**

Plaques with intense expression of **(A)** CD3, **(B)** CD68, and **(C)** vascular endothelial growth factor (VEGF) had higher temperature differences (ΔT).

Table 1 **Demographic Characteristics**

Clinical Variable	Patients (n = 34)	Controls (n = 15)
Age, yrs	73.38 ± 4.77	37.76 ± 4.34
Male	22 (64.7)	10 (66.6)
Prior neurological symptoms	21 (61.7)	0
Hypertension	25 (73.5)	1 (6.6)
Dyslipidemia	16 (47.1)	0
Diabetes	9 (26.4)	0
Smoking	23 (67.6)	4 (26.6)
Previous medications		
Aspirin	34 (100)	0
Calcium channel blocker	19 (55.8)	0
Beta-blockers	7 (20.5)	0
Statins	34 (100)	0
ACE-I	25 (73.5)	0
ARBs	9 (26.5)	0

Values are mean ± SD or n (%).
ACE-I = angiotensin-converting enzyme inhibitor; ARB = angiotensin receptor blocker.

compared with specimens with an absence of or focal or circumscribed presence of inflammatory cells ($p < 0.01$) (Fig. 3D, Table 3).

Immunohistochemistry. We categorized specimens into 2 groups using a cut-off value of 2 based on the semiquantitative scale for CD3, CD68, and VEGF. Specimens with intense expression of CD3 ($\geq$2) had higher ΔT compared with those with lower expression of CD3 ($p < 0.01$) (Fig. 4A). Accordingly, specimens with intense expression of CD68 ($\geq$2) had higher ΔT compared with those with lower expression of CD68 ($p < 0.01$) (Fig. 4B). Moreover, specimens with intense expression of VEGF reactivity ($\geq$2) had higher ΔT compared with those with low VEGF reactivity (<2) ($p < 0.01$) (Fig. 4C, Table 4). For demonstrative purposes of the method, 2 representative cases are shown in Figure 5 and the respective histological segments in Figure 6.

Table 2 **Comparative Evaluation of Ultrasound Plaque Characteristics With Increased Plaque Thermal Difference**

Ultrasound Characteristics (N = 34)	ΔT	°C	p Value
Plaque texture			
Calcified	13 (38.2)	0.96 ± 0.22	<0.01
Fatty	15 (44.1)	1.78 ± 0.41	
Mixed	6 (17.6)	1.38 ± 0.30	
Plaque surface			
Regular	13 (38.2)	0.95 ± 0.19	<0.01
Irregular	12 (35.2)	1.38 ± 0.23	
Ulcerated	9 (26.4)	2.08 ± 0.14	
Plaque echogenicity			
Homogenous	19 (55.8)	1.09 ± 0.31	<0.01
Heterogenous	15 (44.1)	1.78 ± 0.41	

Values are mean ± SD or n (%).
ΔT = temperature difference.

surface had higher ΔT compared with homogenous and irregular and regular surfaces ($p < 0.01$) (Figs. 2B and 2C, Table 2).

Histological analysis. Specimens with increased extension of calcification had lower ΔT compared with specimens with low extension of calcification ($p < 0.01$) (Fig. 3A). Specimens with increased extension of lipid core had higher ΔT compared with specimens with low extension of lipid core ($p < 0.01$) (Fig. 3B). Specimens with thin fibrous caps had higher ΔT compared with specimens with thick fibrous caps (>200 μm) ($p < 0.01$) (Fig. 3C). Specimens with maximal expression of inflammatory cells had higher ΔT

Table 3	Comparative Evaluation of Plaque Histological Features With Increased Plaque Thermal Difference		
Histological Features (N = 34)	**ΔT**	**°C**	**p Value**
Extension of calcification			
0	1 (2.9)	2.00 ± 0.00	<0.01
I	4 (11.7)	1.80 ± 0.41	
II	17 (50)	1.52 ± 0.46	
III	7 (20.5)	1.03 ± 0.44	
IV	5 (14.7)	1.06 ± 0.21	
Extension of the lipid core			
I	14 (41.1)	1.08 ± 0.36	<0.01
II	10 (29.4)	1.48 ± 0.46	
III	6 (17.6)	1.70 ± 0.39	
IV	4 (11.7)	1.85 ± 0.52	
Fibrous cap			
>200 μm	14 (41.1)	0.98 ± 0.20	<0.01
≤200 μm	20 (58.8)	1.69 ± 0.42	
Inflammatory infiltrate			
Yes	18 (52.9)	1.74 ± 0.40	<0.001
No	16 (47.0)	1.01 ± 0.21	

Values are mean ± SD or n (%).
ΔT = temperature difference.

Discussion

The main results of the current study are: 1) ΔT of the carotid atheromatic plaques can be measured in vivo noninvasively by MR; and 2) the in vivo temperature measurements by MR correlate well with the ultrasound characteristics and histological and immunohistochemical findings.

Recent studies have suggested that patients with carotid artery disease and vulnerable atherosclerotic plaques have worse prognosis compared with patients with stable plaques (25,26). The characteristics of these plaques include large lipid core, thin fibrous cap, increased infiltration of inflammatory cells, and neovascularization (5,27). Previous studies showed that inflammation within the atherosclerotic plaques is correlated with thermal heterogeneity (7,28,29). Despite the advancements of imaging methods, currently there is no method for the in vivo noninvasive measurement of carotid plaque temperature (10,12,30).

MR can detect natural electromagnetic radiation from internal tissues at microwave frequencies; because the intensity of the radiation is proportional to the temperature of tissue, MR can provide accurate temperature measurements (14,17,23). Therefore, MR can measure temperature of tissues at a depth of 1 to 7 cm from the skin. Indeed, in an experimental atherosclerotic model, MR provided temperature measurements of hypercholesterolemic rabbit aortas noninvasively, confirmed by intravascular temperature measurements and inflammatory activation observed by histology (18).

Specific comments. The calibration of the MR system was performed by an infrared sensor applied on the skin of the examined subject. Because the temperatures of the skin were lower than the temperatures of the internal tissues, ΔTs

were provided rather than absolute temperature values, as shown for demonstrative purposes in Figure 5. In addition, MR cannot measure an isolated spot within the volume under investigation because the microwave sensor obtains temperature from the whole volume under investigation. Therefore, the maximal temperature at each measurement was underestimated, and consequently, the calculated ΔT was underestimated. Moreover, the maximal penetration depth varies depending on the different dielectric properties of the underlying tissues and on the wavelength used (13). In the present study, the measurements in both groups were performed under the same conditions, and thus, the increased ΔT found in patients with carotid plaques can only be attributed to the atheromatic plaque.

We included patients with severe carotid artery disease to investigate the correlation between MR measurements with morphological plaque characteristics. The distance from the MR antenna to the carotid arteries is <7 cm, especially with gentle pressure on the antenna. Although increased ΔT was found in all diseased carotids (>0.20°C), plaques with "vulnerable" plaque characteristics in the ultrasound examination, including fatty or mixed, ulcerated plaques with heterogeneous morphology, had increased ΔT. These findings were confirmed by the histological and immunohistochemical analysis because plaques with large lipid core, thin fibrous caps, and increased inflammatory density had higher ΔTs compared with calcified plaques with less inflammation.

During thermographic measurements of the target segment, we cannot exclude the possibility of overlapping. However, the entire target segment was scanned, and the thermographic measurements were not affected. Moreover, because we included patients with a single stenosis at the level of the carotid bulb, the interference of other atherosclerotic lesions on MR measurements was diminished. In the case of diffuse carotid artery inflammatory activation, our results may have been underestimated because the reference (minimal) temperature of "healthy" segments would be increased. The possible impact of other adjacent tissues on the measurements of temperature seems limited because the control group had a trivial ΔT.

Table 4	Comparative Evaluation of Plaque Immunohistological Features With Increased Plaque Thermal Difference		
Immunohistological Features (N = 34)	**ΔT**	**°C**	**p Value**
CD68			
High	21 (61.7)	1.67 ± 0.41	<0.01
Low	13 (38.2)	0.95 ± 0.20	
CD3			
High	21 (61.7)	1.66 ± 0.43	<0.01
Low	13 (38.2)	0.98 ± 0.21	
VEGF			
High	17 (50)	1.70 ± 0.48	<0.01
Low	17 (50)	1.09 ± 0.28	

Values are mean ± SD or n (%).
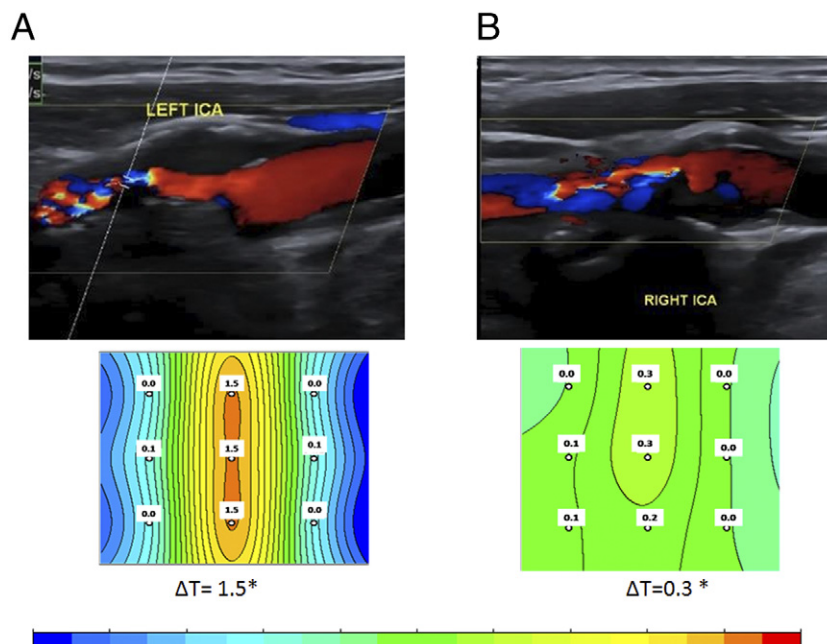ΔT = temperature difference; VEGF = vascular endothelial growth factor.

Figure 5   Representative Ultrasound Images and Corresponding Temperature Fields of 2 Carotid Artery Plaques

Both temperature fields **(lower panels)** represent temperature variations, with cold areas displayed by "cold" colors (i.e., blue) and hot areas by "warm" colors (i.e., red) (temperature scale at the bottom of the figure). The isotherm lines are drawn through sites with the same temperature. After the temperatures were measured, the site with the lowest temperature was assigned to have temperature difference (ΔT) of 0°C, and each temperature measurement was assigned a corresponding ΔT. The temperature fields were obtained after 3 measurements of temperature (perpendicular axis) in each of the 3 carotid segments (horizontal axis). The displayed measurements were obtained by a single operator. **A (upper panel)** shows the ultrasound image of a fatty atherosclerotic plaque, with irregular surface, low echogenicity, and ΔT of 1.5°C **(lower panel)**. **B (upper panel)** shows the ultrasound image of a calcified atherosclerotic plaque with regular surface and ΔT of 0.3°C **(lower panel)**. ICA = internal carotid artery.

Study limitations. MR appears to be an indirect indicator of atherosclerotic plaque inflammatory cell content and does not directly measure inflammatory density; instead, it likely represents an aggregate of multiple consequences of the inflammatory process—namely, increased neovasculature content and inflammation. However, all of the aforementioned parameters are markers of plaque vulnerability providing important clinical information.

Clinical implications. MR may ultimately allow the noninvasive detection of plaque inflammation in vivo. MR may be potentially used to identify patients with a moderate degree of carotid artery stenosis who might benefit from closer monitoring, more aggressive medical therapy, or early intervention. The combined prognostic value of an imaging method with MR needs to be studied. In the current study, in 21% of the plaques without any ultrasound criteria for vulnerability, high temperature was found in accordance with the histology. The improvement of the current MR device may provide information on the natural history of atheromatosis.

Conclusions

In vivo noninvasive measurement of the temperature of carotid atherosclerotic plaques by MR can be performed safely. This new method provides temperature measurements of carotid plaques, reflecting the inflammatory activation within the plaque. This study justifies the performance of prospective clinical studies for the investigation of the prognostic value of temperature difference in carotid artery disease.

Reprint requests and correspondence: Dr. Konstantinos Toutouzas, First Department of Cardiology, Hippokration Hospital, 26 Karaoli and Dimitriou str., Holargos, 15562, Athens, Greece. E-mail: ktoutouz@otenet.gr.

REFERENCES

1. Abbott AL, Bladin CF, Levi CR, Chambers BR. What should we do with asymptomatic carotid stenosis? Int J Stroke 2007;2:27–39.
2. Chaturvedi S, Bruno A, Feasby T, et al. Carotid endarterectomy—an evidence-based review: report of the Therapeutics and Technology Assessment Subcommittee of the American Academy of Neurology. Neurology 2005;65:794–801.
3. Liapis CD, Bell PR, Mikhailidis D, et al. ESVS guidelines. Invasive treatment for carotid stenosis: indications, techniques. Eur J Vasc Endovasc Surg 2009;37:1–19.
4. Hobson RW 2nd, Mackey WC, Ascher E, et al. Management of atherosclerotic carotid artery disease: clinical practice guidelines of the Society for Vascular Surgery. J Vasc Surg 2008;48:480–6.
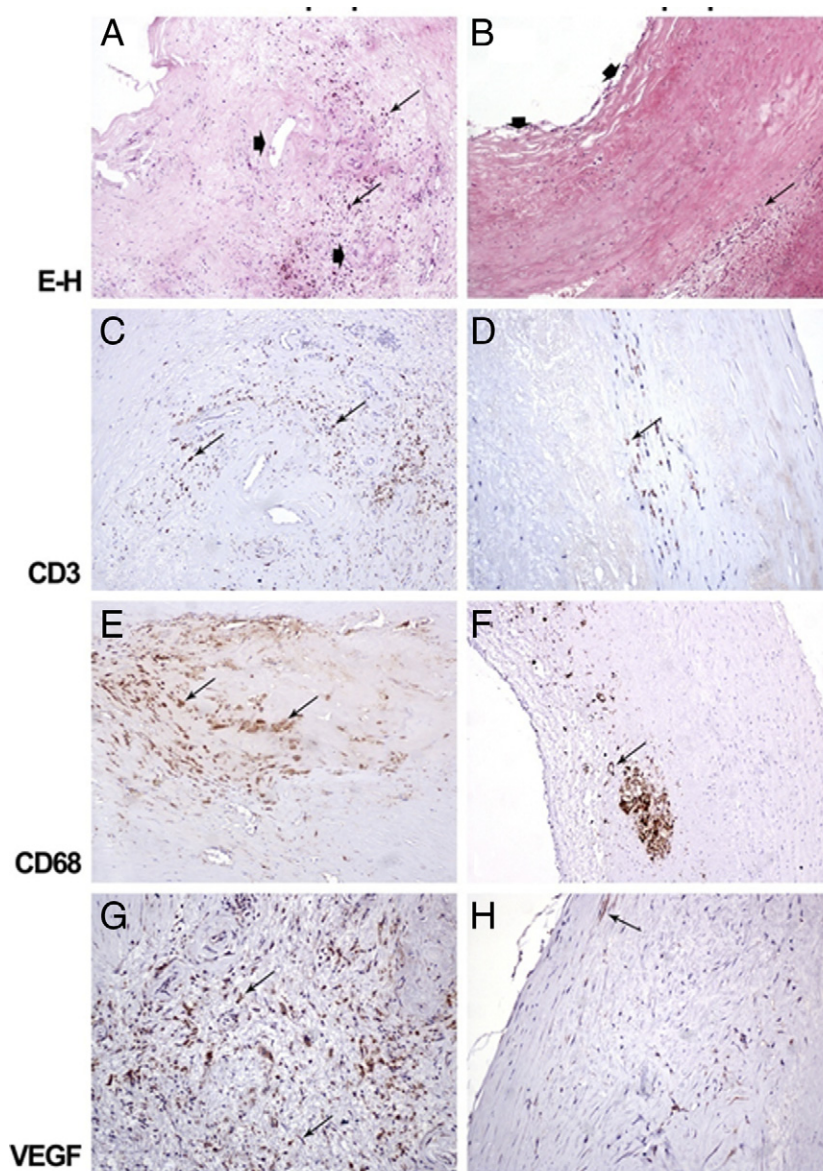
Figure 6   Corresponding Histological and Immunohistochemical Photomicrographs of Plaques

The photomicrographs correspond to the ultrasound and temperature findings presented in Figures 5A and 5B, respectively. **Left columns** correspond to a plaque with increased lipid pool and thin fibrous cap. **Right columns** correspond to a plaque with dense calcification and thick fibrous cap. **(A)** Increased versus **(B)** low expression of inflammatory cell density **(arrows)**. **(C)** Intense versus **(D)** low expression of CD3 **(arrows)**. **(E)** Intense versus **(F)** low expression of CD68 **(arrows)**. **(G)** Intense versus **(H)** low expression of vascular endothelial growth factor (VEGF) **(arrows)**. H-E = hematoxylin and eosin.

5. Virmani R, Ladich ER, Burke AP, Kolodgie FD. Histopathology of carotid atherosclerotic disease. Neurosurgery 2006;59:S219–27, discussion S3–13.
6. Libby P. Inflammation in atherosclerosis. Nature 2002;420:868–74.
7. Casscells W, Hathorn B, David M, et al. Thermal detection of cellular infiltrates in living atherosclerotic plaques: possible implications for plaque rupture and thrombosis. Lancet 1996;347:1447–51.
8. Faggioli GL, Pini R, Mauro R, et al. Identification of carotid 'vulnerable plaque' by contrast-enhanced ultrasonography: correlation with plaque histology, symptoms and cerebral computed tomography. Eur J Vasc Endovasc Surg 2011;41:238–48.
9. Papini GD, Di Leo G, Tritella S, et al. Evaluation of inflammatory status of atherosclerotic carotid plaque before thromboendarterectomy using delayed contrast-enhanced subtracted images after magnetic resonance angiography. Eur J Radiol 2011;80:e373–80.
10. Diethrich EB, Pauliina Margolis M, Reid DB, et al. Virtual histology intravascular ultrasound assessment of carotid artery disease: the Carotid Artery Plaque Virtual Histology Evaluation (CAPITAL) study. J Endovasc Ther 2007;14:676–86.
11. Feinstein SB. Contrast ultrasound imaging of the carotid artery vasa vasorum and atherosclerotic plaque neovascularization. J Am Coll Cardiol 2006;48:236–43.
12. Lombardo A, Rizzello V, Natale L, et al. Magnetic resonance imaging of carotid plaque inflammation in acute coronary syndromes: a sign of multisite plaque activation. Int J Cardiol 2009;136:103–5.
13. Barrett AH, Myers PC. Microwave thermography: a method of detecting subsurface thermal patterns. Bibl Radiol 1975:45–56.

14. Barrett AH, Myers PC, Sadowsky NL. Microwave thermography in the detection of breast cancer. AJR Am J Roentgenol 1980;134:365–8.

15. Shaeffer J, El-Mahdi AM, Carr KL. Cancer detection studies using a 4.7 Gigahertz radiometer. Cancer Detect Prev 1981;4:571–8.

16. Shaeffer J, El-Mahdi AM, Carr KL. Thermographic detection of human cancers by microwave radiometry. Prog Clin Biol Res 1982; 107:509–21.

17. Helmy A, Holdmann M, Rizkalla M. Application of thermography for non-invasive diagnosis of thyroid gland disease. IEEE Trans Biomed Eng 2008;55:1168–75.

18. Toutouzas K, Grassos H, Synetos A, et al. A new non-invasive method for detection of local inflammation in atherosclerotic plaques: experimental application of microwave radiometry. Atherosclerosis 2011;215:82–9.

19. Pearson TA, Blair SN, Daniels SR, et al. AHA guidelines for primary prevention of cardiovascular disease and stroke: 2002 update: Consensus Panel Guide to Comprehensive Risk Reduction for Adult Patients Without Coronary or Other Atherosclerotic Vascular Diseases. American Heart Association Science Advisory and Coordinating Committee. Circulation 2002;106:388–91.

20. Geroulakos G, Ramaswami G, Nicolaides A, et al. Characterization of symptomatic and asymptomatic carotid plaques using high-resolution real-time ultrasonography. Br J Surg 1993;80:1274–7.

21. Bluth EI, Kay D, Merritt CR, et al. Sonographic characterization of carotid plaque: detection of hemorrhage. AJR Am J Roentgenol 1986;146:1061–5.

22. Saba L, Sanfilippo R, Montisci R, Atzeni M, Ribuffo D, Mallarini G. Vulnerable plaque: detection of agreement between multi-detector-row CT angiography and US-ECD. Eur J Radiol 2011; 77:509–15.

23. Barrett AH, Myers PC. Subcutaneous temperatures: a method of noninvasive sensing. Science 1975;190:669–71.

24. Ciccone MM, Marzullo A, Mizio D, et al. Can carotid plaque histology selectively predict the risk of an acute coronary syndrome? Int Heart J 2011;52:72–7.

25. Rundek T, Arif H, Boden-Albala B, Elkind MS, Paik MC, Sacco RL. Carotid plaque, a subclinical precursor of vascular events: the Northern Manhattan Study. Neurology 2008;70:1200–7.

26. Dunmore BJ, McCarthy MJ, Naylor AR, Brindle NP. Carotid plaque instability and ischemic symptoms are linked to immaturity of microvessels within plaques. J Vasc Surg 2007;45:155–9.

27. Krupinski J, Font A, Luque A, Turu M, Slevin M. Angiogenesis and inflammation in carotid atherosclerosis. Front Biosci 2008;13: 6472–82.

28. Madjid M, Naghavi M, Malik BA, Litovsky S, Willerson JT, Casscells W. Thermal detection of vulnerable plaque. Am J Cardiol 2002;90: 36L–9L.

29. Stefanadis C, Diamantopoulos L, Vlachopoulos C, et al. Thermal heterogeneity within human atherosclerotic coronary arteries detected in vivo: a new method of detection by application of a special thermography catheter. Circulation 1999;20;99:1965–71.

30. Coli S, Magnoni M, Sangiorgi G, et al. Contrast-enhanced ultrasound imaging of intraplaque neovascularization in carotid arteries: correlation with histology and plaque echogenicity. J Am Coll Cardiol 2008;52:223–30.

Key Words: atherosclerosis ■ carotid stenosis ■ diagnosis ■ inflammation ■ microwave radiometry.